of the proposed structure is the same as that of a conventional 50 Ω line. The reflection loss of the proposed structure is observed to be less than 10 dB; this can be controlled by adjusting the dimensions of the periodic structure. Fig. 3 shows the slow-wave factor of this perforated microstrip in conjunction with that of a conventional microstrip. The slow-wave factor of the perforated microstrip is 1.2 times higher than that of the conventional microstrip. The slow-wave is generated because inductance of the transmission is increased. We believe that the slow-wave factor can be enlarged further by controlling the inductive section in the periodic structure. The quality factor of the perforated microstrip is compared with that of the conventional microstrip in Fig. 4. The quality-factor ($= \beta/2\alpha$) is 1.17 times higher than that of the conventional microstrip at frequencies lower than 7 GHz. The high Q-factor is generated because the slow-wave factor of the perforated microstrip is increased.

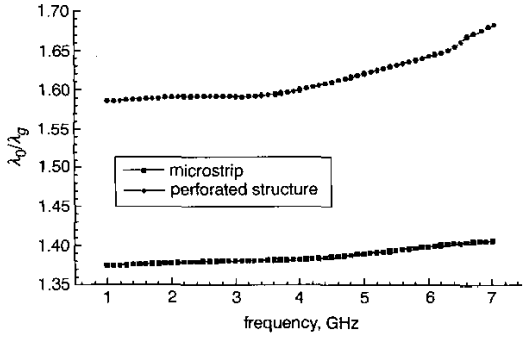

Fig. 3 *Slow-wave factor of perforated slow-wave structure compared with conventional microstrip*

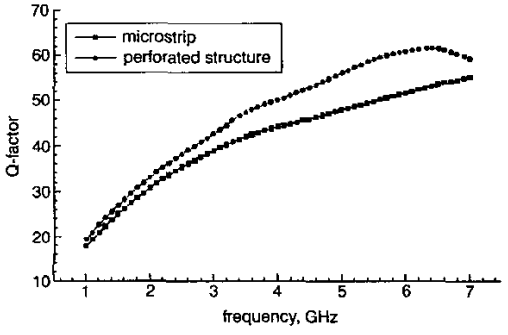

Fig. 4 *Quality factor of perforated slow-wave structure compared with conventional microstrip*

We analysed the proposed perforated slow-wave microstrip and compared the results with a conventional microstrip and periodic geometry modulation microstrip in Table 1. The proposed perforated slow-wave microstrip shows a good matching condition ($Z_0 = 60\ \Omega$) compared to the periodic geometry modulation microstrip ($Z_0 = 75\ \Omega$). At 7 GHz, the perforated microstrip shows a high slow-wave factor of 2.03 compared to the conventional microstrip (1.40) and has improvement of the propagation loss compared to the periodic geometry modulation microstrip.

Table 1: Calculated characteristics of various microstrips at 7 GHz

Type of microstrip	Equivalent Z_0 (Ω)	Attenuation loss (dB/cm)	Slow-wave factor
Conventional microstrip	50	0.030	1.400
Modulated microstrip	76	0.100	1.725
Perforated microstrip	61	0.048	2.030

Conclusions: We have proposed a perforated slow-wave microstrip and characterised it theoretically and experimentally up to 7 GHz. The proposed structure shows 1.2 and 1.17 improvement of the slow-wave factor and quality factor, respectively. The proposed slow-wave perforated microstrip shows good transmission characteristics and matching condition. The perforated microstrip can be applied to a delay line and microwave passive device packages in order to reduce the physical length.

25 March 2002
Electronics Letters Online No: 20020535
DOI: 10.1049/el:20020535

Gye-An Lee and F. De Flaviis (*Department of Electrical and Computer Engineering, University of California at Irvine, Irvine, CA 92697, USA*)

E-mail: gyeanl@uci.edu

Hai-Young Lee (*School of Electronics Engineering, Ajou University, 5 Wonchon-dong, Paldal-ku, Suwon 442-749, Korea*)

References

1 HASEGAWA, H., FURUKAWA, M., and YANAI, H.: 'Properties of microstrip line on Si-SiO_2 system', *IEEE Trans. Microw. Theory Tech.*, 1971, **19**, pp. 869–881
2 MU, T.C., OGAWA, H., and ITOH, T.: 'Characteristics of multiconductor, asymmetric, slow-wave microstrip transmission line', *IEEE Trans. Microw. Theory Tech.*, 1986, **34**, pp. 1471–1477
3 SEKI, S., and HASEGAWA, H.: 'Cross-tie slow-wave coplanar waveguide on semi-insulating GaAs substrate', *Electron. Lett.*, 1981, **17**, pp. 940–941
4 LEE, H.Y., WANG, T.H., and ITOH, T.: 'Confirmation of slow waves in a crosstie overlay coplanar waveguide and its applications to band-reject gratings and reflectors', *IEEE Trans. Microw. Theory Tech.*, 1988, **36**, pp. 1811–1818
5 HONG, J.S., and LANCASTER, M.J.: 'Capacitively loaded microstrip loop resonator', *Electron. Lett.*, 1993, **30**, pp. 1494–1495

Using buried capacitor in LTCC-MLC balun

Ching-Wen Tang and Chi-Yang Chang

A novel chip-type ceramic balun designed in the 2.4 GHz ISM band frequency is presented. A buried capacitor is included in the balun, so that the length of the coupled transmission lines can be reduced and can be designed very easily. A meander or spiral broadside coupled-line is adopted to realise the proposed LTCC multi-layer balun. The measured performances of phase and amplitude balance for this LTCC-MLC balun show a good match with computer simulation.

Introduction: Low temperature co-fired ceramic (LTCC) multi-layer ceramic (MLC) technology is widely used to realise a high performance RF front-end for wireless applications because it is suitable for the realisation of integrated passive components and for interconnection with active devices. It enables the miniaturisation of RF telecommunication devices for portable and battery-powered applications, reduces size, weight, cost and power consumption and is becoming essential in the current trend. Among those passive RF components used in modern wireless communications, the balun is one of the most important, since it can be used in double-balanced mixer and push-pull amplifier design. It provides balanced outputs from an unbalanced input.

Many types of balun have been proposed such as the active [1], the lumped-type [2], toroid-type [3], and magic-T hybrid baluns [4]. However, for various different reasons, these baluns do not meet the requirements described previously. In contrast, the LTCC balun [5–7] can.

In this Letter, we propose new multi-layer structure to realise the chip type LTCC balun. By using a buried capacitor in the LC resonator, the length of a coupled strip-line can be shortened accordingly. This new multi-layer balun exhibits a good balanced characteristic. The calculated and measured response of the proposed LTCC-MLC balun shows superior performances.

Design procedure: There are several methods to shorten the transmission line [5–9]. Fig. 1 shows the new multi-layer structure to realise the proposed LTCC-MLC balun. Its equivalent circuit is shown in Fig. 2. The input and output resonant circuits are both formed by a transmission line in parallel with a capacitor. The length of the output

transmission line is longer than the input transmission line and the full length of the input transmission line is coupled to a part of the output transmission line via the broadside coupling structure as shown in Fig. 1. The design procedures are described in [7].

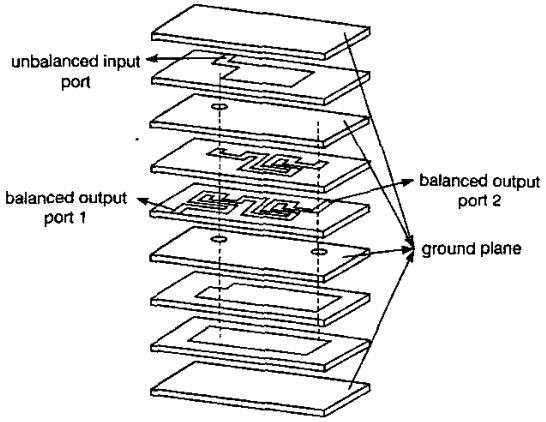

Fig. 1 *Proposed multi-layer structure of LTCC-MLC balun*

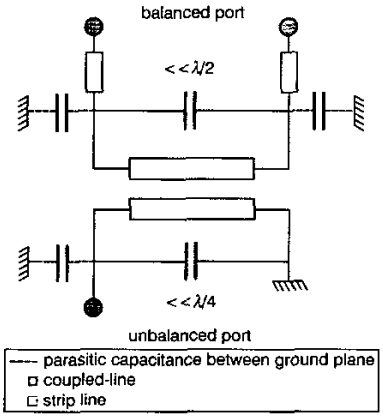

Fig. 2 *Equivalent circuit of LTCC-MLC balun*

Simulated and measured results: This chip type balun is designed to operate in the 2.4 GHz ISM band frequency. This structure requires two LC resonators to realise the multi-layer balun. The proposed LTCC-MLC balun is shown in Fig. 3. This balun is fabricated with a multi-layer configuration using 90 μm thick ceramic sheets ($\varepsilon_r = 7.8$) and a 10 μm thick Ag metal pattern. The overall size of the balun is 3.2 mm × 1.6 mm × 0.8 mm. The unbalanced input impedance $R_1 = 50\,\Omega$ and the balanced output impedance $R_2 = 50\,\Omega$.

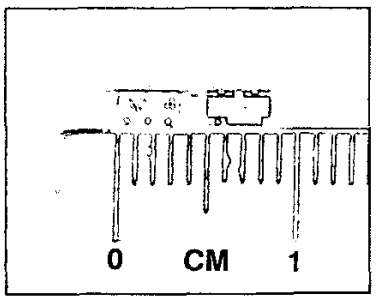

Fig. 3 *Photograph of fabricated LTCC-MLC balun of Fig. 1*

The simulated (based on perfect conductor and lossless dielectric material) and measured results of the balun are shown in Fig. 4. The insertion loss and the return loss are less than −1.3 dB and −13.2 dB, respectively for simulation, −3.2 dB and −12.6 dB, respectively for measurement over the frequency range of 2.34–2.54 GHz as shown in Fig. 4*a*. The amplitude and phase imbalance between balanced outputs are within 2.1 dB and 1.4°, respectively for simulation and 3.4 dB and 2.9°, respectively for measurement over the operating frequency range as shown in Fig. 4*b*. Excellent matching between theoretical and measured results is obtained except for insertion loss. The measured insertion loss is higher than the simulated result because substrate and metal loss are not included in the simulation so as to increase speed.

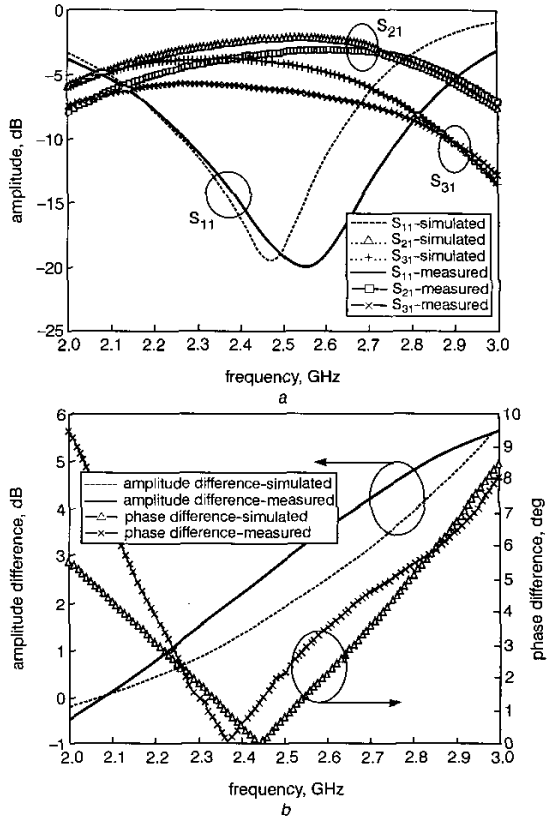

Fig. 4 *Simulated and measured results of LTCC-MLC balun of Fig. 1*
a Insertion loss and return loss
b Amplitude and phase difference between balanced output

Conclusion: A new LTCC-MLC balun has been developed and demonstrated. The design method and the equivalent circuit of this balun have been given. This balun is compact, and measured performance agrees well with computer simulation. The designed chip type balun has been fabricated with a multi-layer configuration. The simulated and measured results show the validity of the proposed design method and the equivalent circuit of the balun.

Acknowledgment: This work was supported in part by the National Science Council, Taiwan, R.O.C., under grant NSC90-2213-E009-033.

6 November 2001
Electronics Letters Online No: 20020586
DOI: 10.1049/el:20020586

Ching-Wen Tang and Chi-Yang Chang (*Department of Communication Engineering, National Chiao Tung University, Hsinchu, Taiwan, R.O.C.*)

E-mail: mhchang@cc.nctu.edu.tw

References

1 TITUS, W.S., and SCHINDLER, M.J.: 'Active balun'. US Patent 4 994 755, 19 February 1991
2 APEL, T.R., and PAGE, C.E.: 'Lumped parameter balun'. US Patent 5 574 411, 12 November 1996
3 ONIZUKA, M., and SATO, K.: 'Balun transformer core material, Balun transformer core and Balun transformer'. US Patent 6 033 593, 7 March 2000

4 MAAS, S.A.: 'Microwave mixers', 2nd edn. (Artech House, Boston, 1993), pp. 244–247

5 FUJIKI, Y., MANDAI, H., and MORIKAWA, T.: 'Chip type spiral broadside coupled directional couplers and baluns using low temperature co-fired ceramic'. Electronic Components and Technology Conference, 1999, pp. 105–110

6 LEW, D.W., PARK, J.S., AHN, D., KANG, N.K., YOO, C.S., and LIM, J.B.: 'A design of the ceramic chip balun using the multilayer configuration', *IEEE Trans. Microw. Theory Tech.*, 2001, **49**, (1), pp. 220–224

7 TANG, C.W., SHEEN, J.W., and CHANG, C.Y.: 'Chip type LTCC-MLC baluns using stepped impedance method', *IEEE Trans. Microw. Theory Tech.*, 2001, **49**, (12), pp. 1–8

8 WINTER, F., TAUB, J., and MARCELLI, M.: 'High-dielectric constant stripline band-pass filters'. Dig. IEEE MTT-S, 1991, pp. 555–556

9 KUMAR, B.P., BRANNER, G.R., and THOMAS, D.G.: 'A reduced size planar balun structure for wireless microwave and RF applications'. Dig. IEEE MTT-S, 1996, pp. 526–529

Vertically periodic defected ground structure for planar transmission lines

J.-S. Lim, C.-S. Kim, Y.-T. Lee, D. Ahn and S. Nam

A vertically periodic defected ground structure (VPDGS) for microstrip. VPDGS has additional vertical periodicity of defects plus the conventional horizontal periodicity on the ground plane. The slow-wave factors and the predicted and measured performances are presented.

Introduction: There has recently been an increasing interest in microstrips combined with periodic structures such as photonic bandgap (PBG) [1] and defected ground structures (DGS) [2]. There have been applications of periodic structures to microwave circuits such as filters [2], power amplifiers [3, 4], and dividers [5]. One of the important properties of PBG and DGS is the increased slow-wave effect, which is caused by the equivalent inductance and capacitance. Hence, transmission lines with very high impedance can be realised and circuit size can be reduced using these properties [5].

The representative feature of the proposed vertically periodic defected ground structure (VPDGS) is that it is possible to organise the periodicity along not only horizontal but also vertical directions, while conventional periodic structures have the only horizontal array [2, 6] or spread structure all over the ground plane [1]. Owing to the vertically periodic structure, a much higher slow-wave factor can be obtained than existing periodic structures for the same physical length of transmission line.

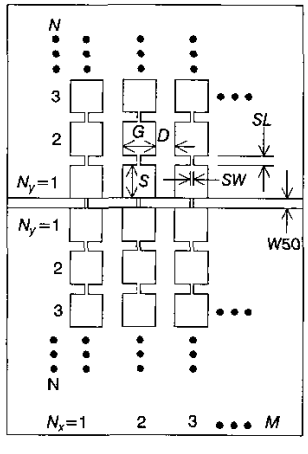

Fig. 1 *Microstrip lines with VPDGSs on ground plane*
a Microstrip
Fr-4, $\varepsilon_r = 4.6$, $H = 0.75$, $W50 = 1.4$, $G = S = 5$, $D = 3$, $SW = 0.5$, $SL = 1.5$
All units are mm

Structure of VPDGS: Fig. 1 shows the structure of the microstrip lines combined with the proposed VPDGS. N_x and N_y mean the number of periodic defects along the horizontal and vertical direction, respectively. The VPDGS is the extended DGS along the vertical direction from the basic structure, which was presented in [2]. The unit DGS element can be expressed as $(N_x, N_y) = (1, 1)$ if the position and the number of DGS elements are expressed as a matrix form for convenience. All dimensions shown in Fig. 1, N_x, and N_y, are determined from the required frequency response.

Slow-wave factors: The slow-wave factors (SWFs) of the microstrip combined with the proposed VPDGS are expected to be greater than those of standard lines because of the additional equivalent L-C components. Fig. 2 shows the SWFs of the microstrip lines with the VPDGS and those of the standard lines with the same physical length up to the first resonance frequency. It is observed that the SWFs have increased greatly by VPDGS. Fig. 2 also shows that the VPDGS with larger N_y for fixed N_x $(=1)$ has lower cutoff frequency and higher SWF.

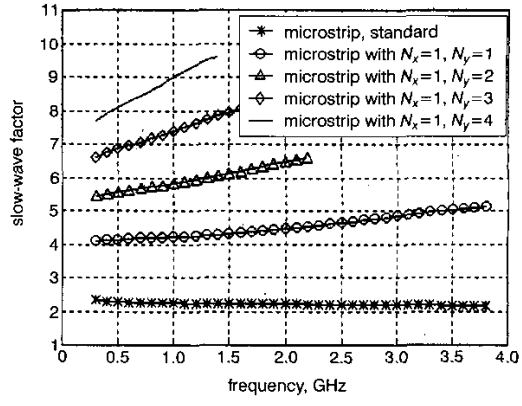

Fig. 2 *Slow-wave factors of microstrip lines with VPDGS and standard lines*

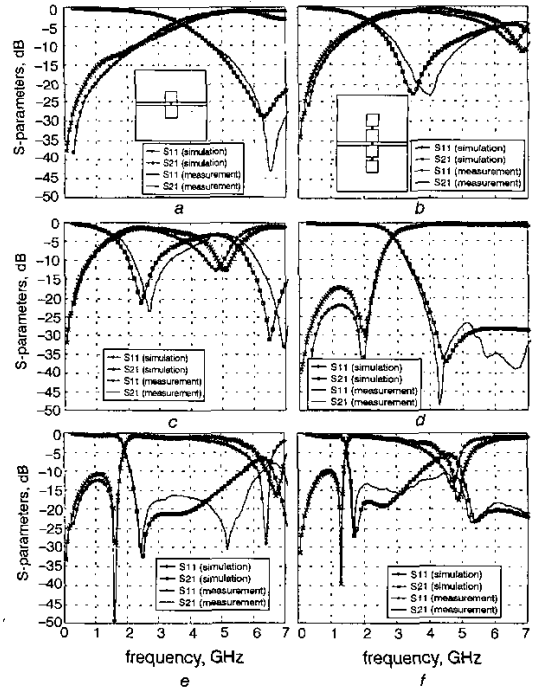

Fig. 3 *Predicted and measured performance of microstrip lines with various matrices of VPDGS*

a (1, 1)
b (1, 2)
c (1, 3)
d (2, 1)
e (2, 2)
f (2, 3)